Supporting Information

Atomic insight into spin, charge and lattice modulations at $SrFeO_{3-x}/SrTiO_3$ interfaces

Kun Xu[a,b], Youdi Gu[c,d], Cheng Song[c], Xiaoyan Zhong*[a,e,f], Jing Zhu*[a,b]
[a]National Center for Electron Microscopy in Beijing, Key Laboratory of Advanced Materials (MOE), The State Key Laboratory of New Ceramics and Fine Processing, School of Materials Science and Engineering, Tsinghua University, Beijing 100084, People's Republic of China.
[b]Central Nano & Micro Mechanism, Tsinghua University, Beijing 100084, People's Republic of China.
[c]Key Laboratory of Advanced Materials (MOE), School of Materials Science and Engineering, Tsinghua University, Beijing 100084, People's Republic of China.
[d]Shenyang National Laboratory for Materials Science, Institute of Metal Research, Chinese Academy of Sciences, Shenyang 110016, People's Republic of China.
[e]Department of Materials Science and Engineering, City University of Hong Kong, Tat Chee Avenue, Kowloon, Hong Kong SAR, People's Republic of China.
[f]Nanomanufacturing Laboratory (NML), City University of Hong Kong Shenzhen Research Institute, Shenzhen 518057, People's Republic of China.

*Corresponding Author: jzhu@mail.tsinghua.edu.cn (J.Z.), xzhong25@cityu.edu.hk (X.Y.Z.)

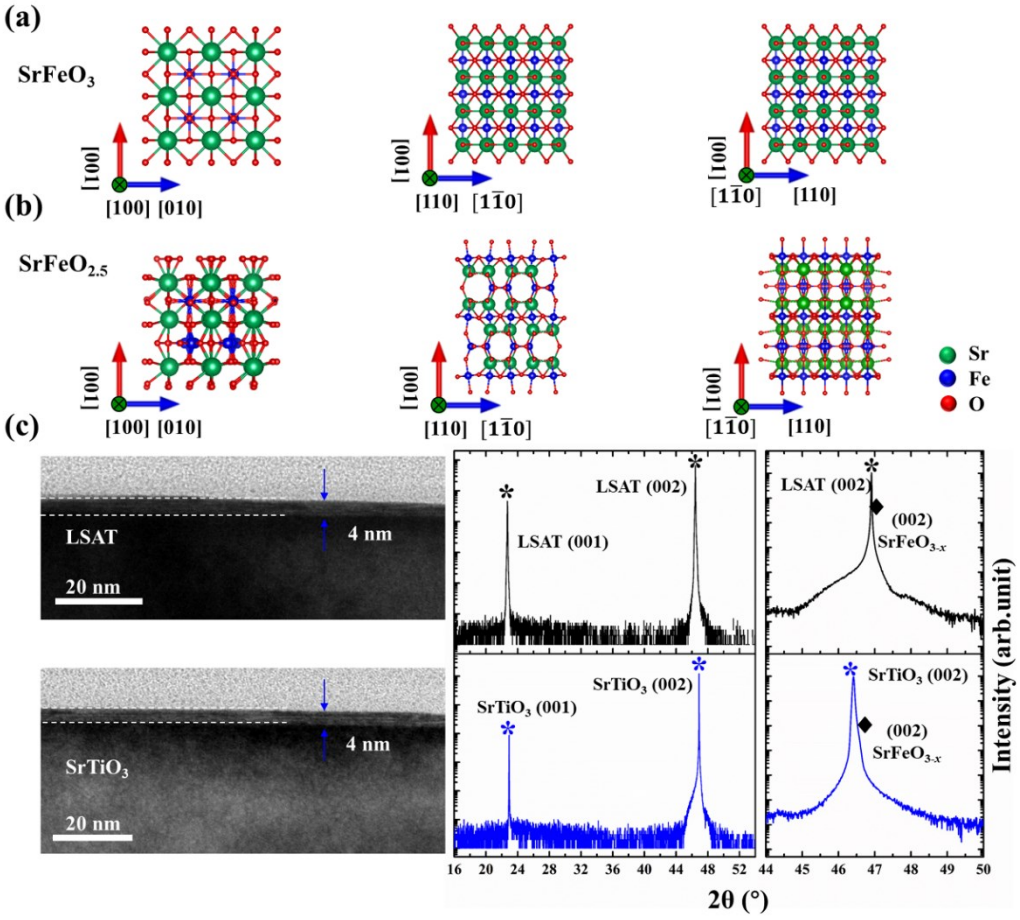

Figure S1. The projected atomic model images of $SrFeO_3$ and $SrFeO_{2.5}$ viewed from different zone axes and XRD structure analysis of 4nm $SrFeO_{3-x}$ films grown on STO and LSAT substrates. (a) $SrFeO_3$ and (b) $SrFeO_{2.5}$ atomic structure models are depicted viewed from [100], [110] and $[1\bar{1}0]$ zone axes respectively. For $SrFeO_{2.5}$ phase, the dumbbell structure can be seen from specific diagonal direction due to ordered oxygen vacancies. (c) XRD results of 4 nm-films grown on $SrTiO_3$ and LSAT substrates, indicating that 4 nm films of $SrFeO_{3-x}$ are coherent to the substrates. The blue (black) star asterisks marks the diffraction planes of $SrTiO_3$ (LSAT), while the diamond asterisks mark the diffraction planes of $SrFeO_{3-x}$.

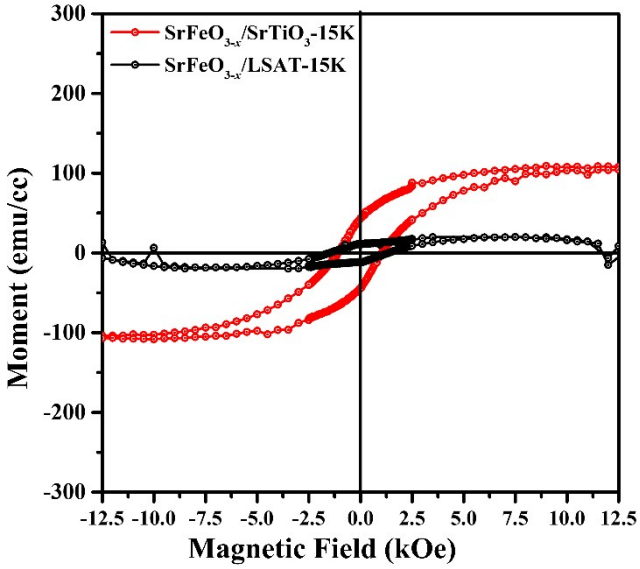

Figure S2. The out of plane magnetic hysteresis loops of 10 nm-$SrFeO_{3-x}/SrTiO_3$ and 10nm-$SrFeO_{3-x}$/LSAT at 15 K, respectively.

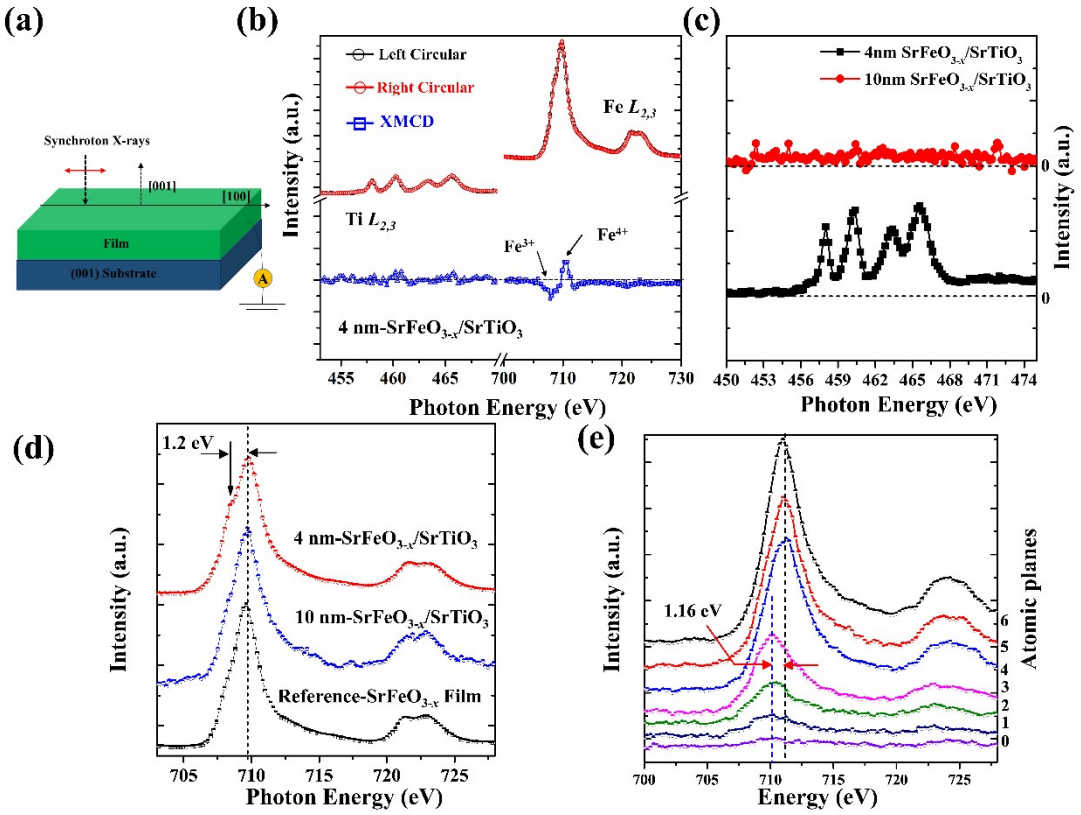

Figure S3. (a) Schematic of the experimental setup for XAS measurements is depicted.

(b) Comparison of XMCD spectra of Ti and Fe $L_{2,3}$ edge for 4 nm-$SrFeO_{3-x}$/$SrTiO_3$. (c) Comparison of Ti $L_{2,3}$ edge for 4 nm and 10 nm- $SrFeO_{3-x}$. It reveals that Ti $L_{2,3}$ signal of region close to interface can be probed in 4nm-$SrFeO_{3-x}$-$SrTiO_3$, while no obvious signal of Ti $L_{2,3}$ can be observed, indicating that interfacial information for 10nm samples cannot be probed by X-ray. (d) Comparison of XAS for Fe $L_{2,3}$ edge in 4 nm-$SrFeO_{3-x}$/$SrTiO_3$, 10 nm- $SrFeO_{3-x}$ and reference $SrFeO_{3-x}$ film sample. The pre-peak feature of Fe L_3 edge can be observed in 4nm $SrFeO_{3-x}$/$SrTiO_3$, while less obvious pre-edge in reference sample is mainly due to the crystal field splitting, whose energy gap is measured to be around 1.6 eV, larger than energy difference ~1.2 eV between pre-peak and main peak observed in 4nm-$SrFeO_{3-x}$/$SrTiO_3$. (e) EELS are acquired on cross-section sample of $SrFeO_{3-x}$/$SrTiO_3$, it reveals that peaks' positions of Fe L_3 edge (marked by blue dotted lines) close to interface shift towards lower energy compared to that away from interface (marked by black dotted line), and this energy position difference is measured around 1.16 eV, which is very close to the energy position difference between pre-peak and L_3 peak measured in (d). Besides, our previous works show that $SrFeO_{3-x}$ films have no additional pre-peak features in L_3 peaks.[1]

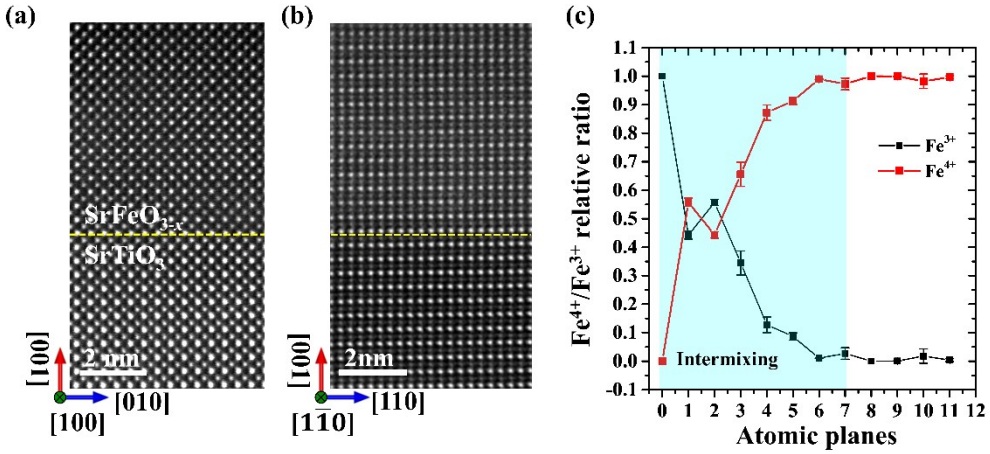

Figure S4. Atomic structure characterization along [100], [1$\bar{1}$0] direction and the Fe^{4+}/Fe^{3+} ratio across the 10 nm-$SrFeO_{3-x}$/$SrTiO_3$ interface. The STEM-HAADF image is shown along the [100] (a) and [1$\bar{1}$0] direction (b). The scale bar is 2 nm. (c) **Figure S4.** Atomic structure characterization along [100], [1$\bar{1}$0] direction and the Fe^{4+}/Fe^{3+} ratio across the 10 nm-$SrFeO_{3-x}$/$SrTiO_3$ interface. The STEM-HAADF image is shown along the [100] (a) and [1$\bar{1}$0] direction (b). The scale bar is 2 nm. (c) By fitting the Fe^{3+}/Fe^{4+} using reference spectra in line scanning EELS in Figure 4c, Fe^{4+}/Fe^{3+} relative ratio is plotted as the function of atomic planes at the interface. Gaussian fitting models

were applied to get weights of Fe^{3+} and Fe^{4+} spectra by fitting line-scanning spectra image of Figure 4c in different atomic planes. Then we could extract a series of weights for Fe^{3+} and Fe^{4+} spectra in neighboring pixels belongs to specific atomic plane, and further calculated the Fe^{4+}/Fe^{3+} relative ratio by using fitting weights of Fe^{3+} and Fe^{4+} spectra. Finally, we could average a series of measured relative ratio between a series of pixels belongs to one atomic plane, and standard error bar could be estimated.

5. Quantitative measurement of (scanning) transmission electron microscopy images

Quantitative analysis of (S)TEM images were performed using the embedded programs in MacTempas. Atomic positions of (S)TEM images were correctly determined by fitting the images' intensity maxima with 2-dimensional Gaussian peaks fitting. The different positions of A-sites or B-sites could be recorded and the intraatomic distance (*a*, *c* constant) could be calculated by averaging them for over twenty-unit cells along the in-plane direction (parallel to the $[100]_{SrTiO3}$ direction). Finally, the recorded STEM-HAADF images were filtered by using wiener filter method in MacTempas.

6. Details about calculation for the moment of each Fe spin in $SrFeO_{3-x}/SrTiO_3$

The calculation details can be seen in the following:

1. As for 4nm-$SrFeO_{3-x}/SrTiO_3$, M_s (Saturation magnetization in 4nm $SrFeO_{3-x}/SrTiO_3$) is estimated to be about 1.05×10^{-5} emu (the contribution from the intermixing area at interfaces defined as $\mu_{Fe(interface)}$ belongs to the intermixing area with the thickness of around 1.6 nm, while the contribution from the bulk regions defined as $\mu_{Fe(bulk)}$ belongs to the region away from interface around 2.4nm).

Due to 1 $\mu_B = 9.274\times10^{-21}$ emu, $V_{SrFeO_3} = 58$ Å^3

$V_{interface}$ = 4mm (film length) × 5mm (film width) × 1.6nm (we estimate the depth of intermixing area according to the profile intensity of EDS and EELS results in Figure S7, around 1.6nm).

So, V_{bulk} = 4mm (film length) × 5mm (film width) × 2.4nm

2. As for 10nm-$SrFeO_{3-x}/SrTiO_3$, M_s (Saturation magnetization in 10nm $SrFeO_{3-x}/SrTiO_3$) is estimated to be about 2.5×10^{-5} emu (contribution from interface defined as $\mu_{Fe(interface)}$ belongs to the intermixing area around 3.2~3.6 nm, while contribution from bulk defined as $\mu_{Fe(bulk)}$ belongs to the region away from interface around 6.4~6.8nm).
$V_{interface}$ = 4mm (film length) × 5mm (film width) × 3.2~3.6nm
So, V_{bulk} = 4mm (film length) × 5mm (film width) × 6.4~6.8nm

Combining equations (1) and data from $SrFeO_{3-x}/SrTiO_3$ with different thickness:

$$\mu_{Fe(interface)} * \frac{V_{interface}}{V_{SrFeO_3}} + \mu_{Fe(bulk)} * \frac{V_{bulk}}{V_{SrFeO_3}} = M_S \quad (1)$$

We can calculate two unknows of $\mu_{Fe(interface)}$ and $\mu_{Fe(bulk)}$ via two equations as shown in (1).

then $\mu_{Fe(interface)}$ can be calculated as 1.1 ~ 1.4 μ_B,

$\mu_{Fe(bulk)}$ can be calculated as 0.40~ 0.62 μ_B

3. To compared with $SrFeO_{3-x}/LSAT$ with different thickness.

We also calculate the spin moment of per Fe atom.

1. as for 4nm SFO/LSAT, $Ms = 0.375\times10^{-5}$ emu,

V= 4mm (film length) × 5mm (film width) × 4nm

$\mu_{Fe(bulk)}$ can be calculated as 0.2931μ_B.

2. as for 10nm SFO/LSAT, $Ms = 1.25\times10^{-5}$ emu

V = 4mm (film length) × 5mm (film width) × 10nm

$\mu_{Fe(bulk)}$ can be calculated as 0.3908 μ_B.

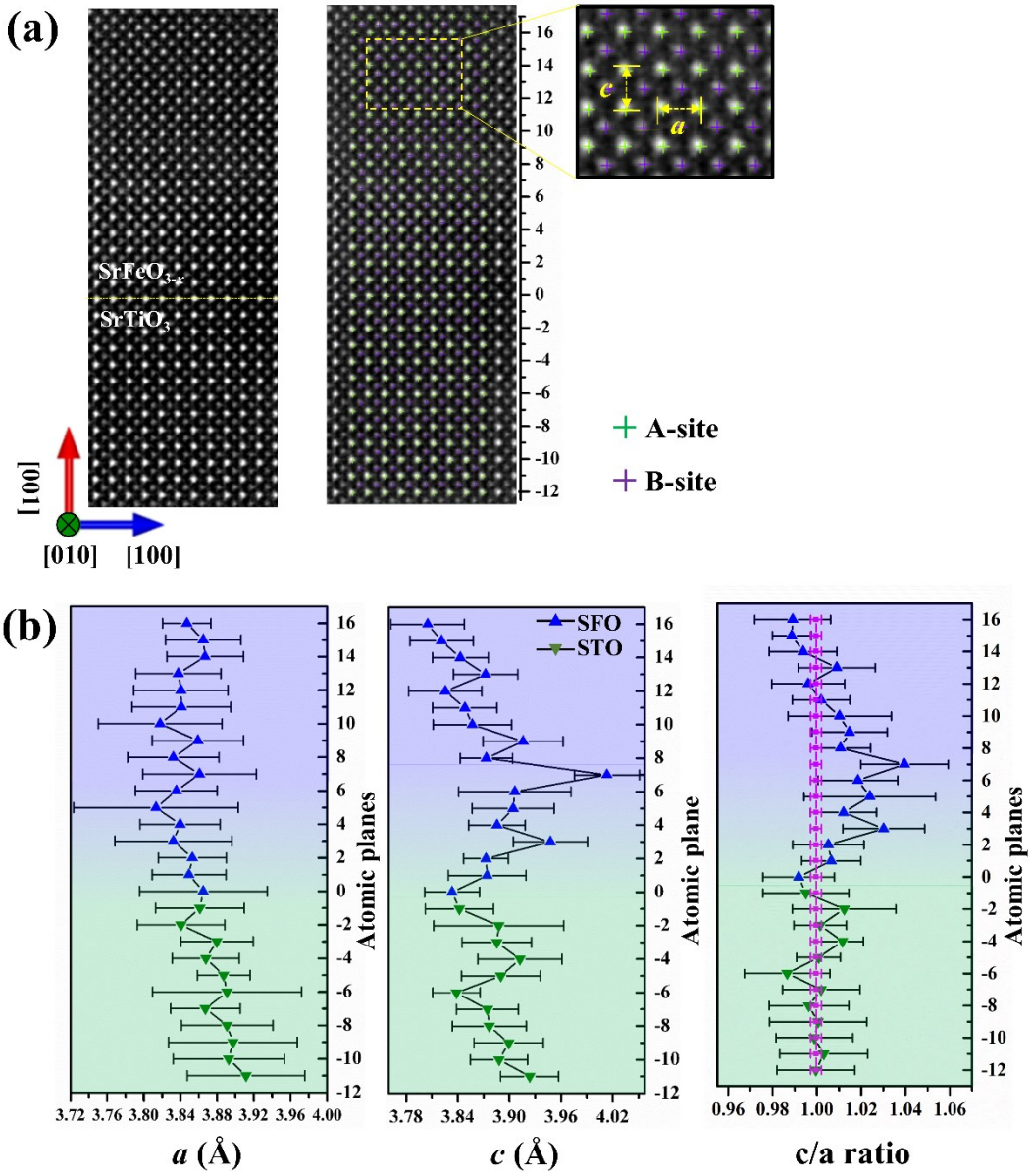

Figure S5. Estimation of the lattice constants. (a) STEM-HAADF image of $SrFeO_{3-x}/SrTiO_3$ sample in the left panel and fitted atom column position superposed in the HAADF image in the right panel with its enlarged view of the boxed region are displayed. The atom positions are determined with the fitted Gaussian models indicated by the cross-shaped symbols. And the lattice constants are estimated from the mean distance between neighboring columns of the A-site atomic columns (red cross-shaped symbol) along the ***a***-and ***c***-direction. (b) The mean lattice constants along the ***a***-direction and ***c***-direction, and ***c***/***a*** ratio as a function of atomic planes across the interface are plotted. We obtain the error bars by calculating the standard deviation values from the measured lattice constants of about 8-unit cells in each layer. The blue and green symbols denote the constants and *c*/*a* ratio of $SrFeO_{3-x}$ and substrate $SrTiO_3$

respectively. The averaged c/a ratio of substrate $SrTiO_3$ (STO) is indicated by magenta horizontal line. The averaged c/a ratios of $SrTiO_3$ were measured to be 0.9996 ± 0.0024 by averaging c/a ratio of atomic planes from -12th to -8th atomic planes.

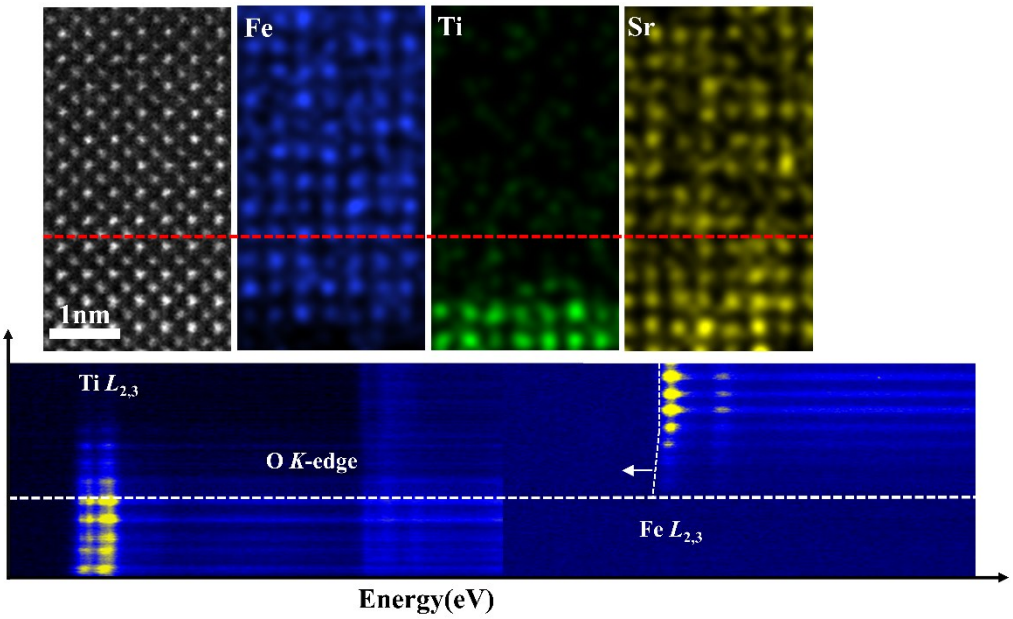

Figure S6. Compositional and valence state analysis for 4 nm-$SrFeO_{3-x}/SrTiO_3$ (a) The false-color Ti (in green), Fe (in blue), Sr (in yellow) EDX elemental maps respectively. The scale bar is 1nm. Ti and Fe signal can be resolved in the area below red line, and intermix with each other. (b)The mapping of electron loss near edge structures of Ti, Fe $L_{2,3}$- and O K-edges at atomic scale respectively. Close to the intermixing area, Fe $L_{2,3}$ edge obviously shifts towards lower energy loss position together with the diminished e_g/t_{2g} splitting features observed in Ti $L_{2,3}$ edge. It can be concluded that the interfacial structure in 4 nm-$SrFeO_{3-x}/SrTiO_3$ is consistent with that observed in 10 nm-$SrFeO_{3-x}/SrTiO_3$. These evidences indicate that the intermixing area in 4 nm -$SrFeO_{3-x}/SrTiO_3$ is around 1.6 nm.

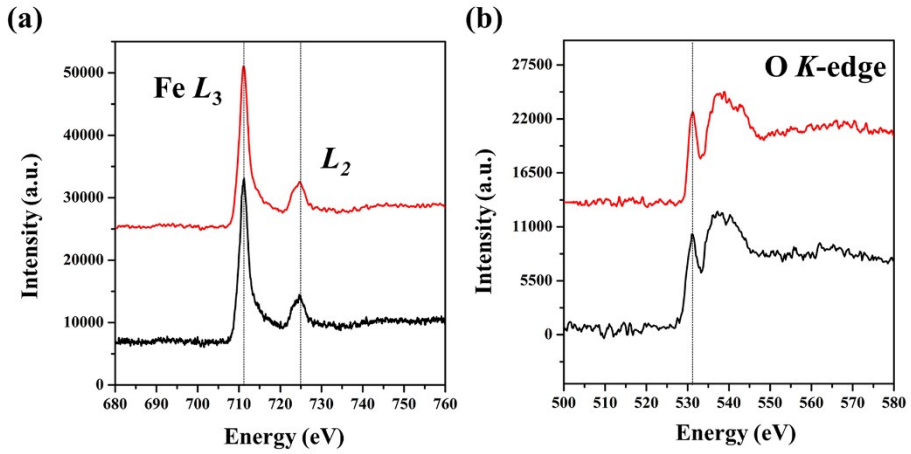

Figure S7. EEL spectra of Fe $L_{2,3}$ edge (a) and O K-edge (b) acquired from the region away from interface for $SrFeO_{3-x}/SrTiO_3$ (plotted with red line) and $SrFeO_{3-x}$/LSAT (plotted with black line) heterojunctions respectively. The calculated white ratios of Fe $L_{2,3}$ edge is 3.812 for $SrFeO_{3-x}/SrTiO_3$ heterojunction and 3.859 for $SrFeO_{3-x}$/LSAT heterojunction and O K-edge shows the similar features compared with each spectrum, it indicates that the film $SrFeO_{3-x}$ grown on different substrates away from the interface almost have the same composition with Fe/O ratio.

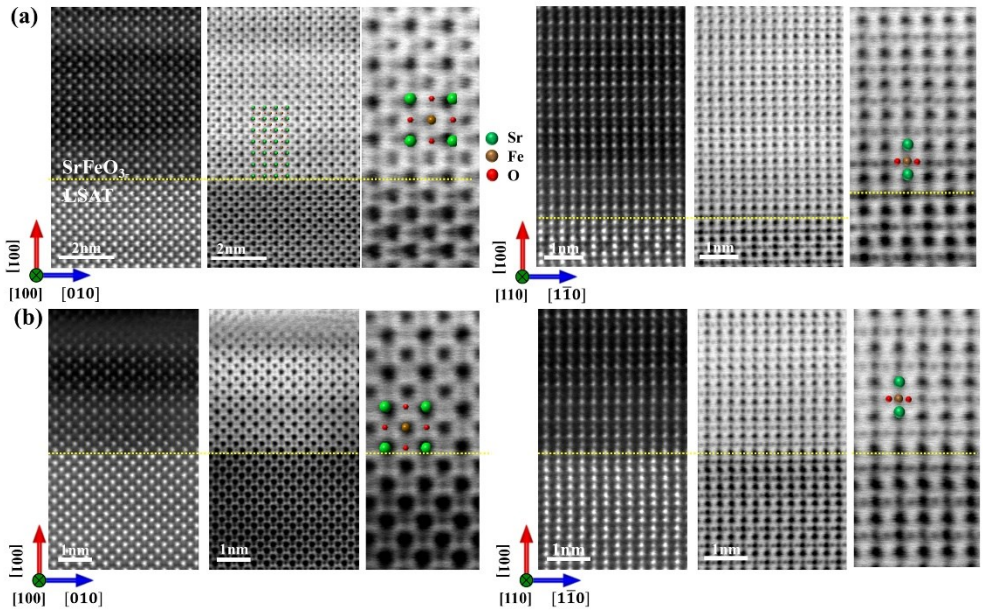

Figure S8. (a) The STEM-HAADF and ABF images across the 10 nm-$SrFeO_{3-x}$/LSAT heterointerface along the [100] and [110] direction respectively. The orange lines identify the interface. Atomic model with oxygen arrangement is consistent with experimental result in ABF image. Enlarged view of ABF images superimposed by atomic models are extracted from middle ABF images, clearly showing the consistent

oxygen atomic arrangements. (b) The STEM-HAADF and ABF images across the 4 nm-$SrFeO_{3-x}$/LSAT heterointerface along the [100] and [110] direction respectively.

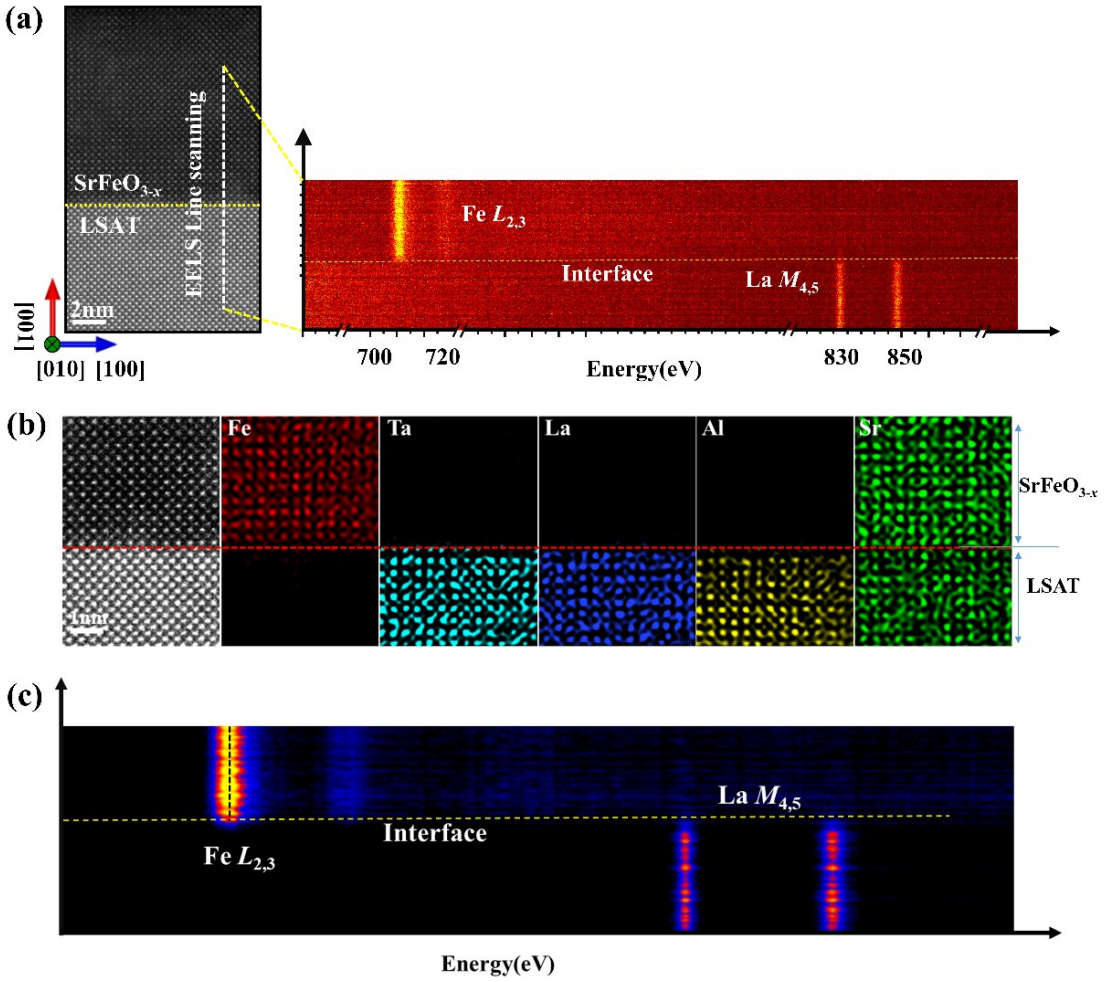

Figure S9. (a) the atomic-plane resolved mapping of ELNES of Fe $L_{2,3}$- and La $M_{4,5}$ – edges are acquired from the region marked with white line in the left STEM-HAADF image along the [001] direction for 10 nm-$SrFeO_{3-x}$/LSAT. (b) The false-color Fe, Ta, La, Al, Sr EDX elemental maps of 4 nm- $SrFeO_{3-x}$/LSAT, respectively. EDS map shows that interface is sharp without obvious element intermixing. (c) EELS line scanning across interface of 4 nm-$SrFeO_{3-x}$/LSAT indicates that there is no valence change and elements intermixing.

Reference:

1. M. S. Saleem, B. Cui, C. Song, Y. Sun, Y. Gu, R. Zhang, M. U. Fayaz, X. Zhou, P. Werner and S. S. Parkin, *ACS Appl. Mater. Interfaces*, 2019, **11**, 6581-6588.